

## Nucleon helicity asymmetries in quasielastic neutrino-nucleus interactions

P. Lava, N. Jachowicz, M. C. Martínez, and J. Ryckebusch\*

*Department of Subatomic and Radiation Physics, Ghent University, Proeftuinstraat 86, B-9000 Gent, Belgium*

(Received 1 March 2006; published 23 June 2006)

We investigate the helicity properties of the ejectile in quasielastic neutrino-induced nucleon-knockout reactions and consider the  $^{12}\text{C}$  target as a test case. A formalism based on a relativistic mean-field model is adopted. The influence of final-state interactions is evaluated within a relativistic multiple-scattering Glauber approximation model. Our calculations reveal that the nucleon helicity asymmetries  $A_l$  in quasielastic  $A(\nu, N)$  and  $A(\bar{\nu}, N)$  reactions are hardly affected by medium corrections, as final-state interactions and off-shell ambiguities in the electroweak current operators. On the contrary, the values of  $A_l$  in  $A(\bar{\nu}, N)$  processes are extremely sensitive to strange-quark contributions to the weak vector form factors.

DOI: [10.1103/PhysRevC.73.064605](https://doi.org/10.1103/PhysRevC.73.064605)

PACS number(s): 25.30.Pt, 24.10.Jv, 24.70.+s, 14.20.Dh

### I. INTRODUCTION

Recently, nucleon polarization properties have been put forward as a potential tool to discriminate between neutrinos and antineutrinos in neutral-current (NC) neutrino-induced nucleon-knockout reactions off nuclei [1,2]. It was shown that neutrinos favor the emission of nucleons with their spin antiparallel to their momentum, whereas the opposite behavior is observed for antineutrinos. Accordingly, the nucleon helicity asymmetry  $A_l$ —defined as the difference in strength for the two possible longitudinal ejectile polarizations, normalized to the total nucleon-knockout cross section—turned out to be very large and of opposite sign for neutrinos and antineutrinos. The theoretical predictions of Refs. [1,2] for this helicity asymmetry were obtained in a nonrelativistic plane-wave impulse approximation (NRPWIA) for neutrino beam energies up to 500 MeV.

Current experimental neutrino research shows a tendency toward higher neutrino energies. In the few GeV regime, any realistic model requires the inclusion of relativity, not only in the kinematics but also in the dynamics of the process. In this work, the nucleon helicity asymmetry  $A_l$  is studied within the relativistic multiple-scattering Glauber approximation (RMSGGA) [3]. Initially developed for the description of exclusive  $A(e, e'p)$  reactions, this model has been recently applied to compute quasielastic neutrino-nucleus cross sections from medium to high neutrino energies [4]. First, we wish to investigate the sensitivity of the above-mentioned selectivity properties of  $A_l$  to the inclusion of various medium effects that were neglected in the model of Refs. [1,2]. We focus on the influence of typical medium effects such as final-state interactions (FSI) and off-shell ambiguities. In addition, our fully relativistic model allows to probe higher energies.

It will be shown that the nucleon helicity asymmetry, which is after all a ratio of cross sections, is only marginally affected by the abovementioned medium-related corrections. Hence, one may be tempted to address more exotic effects, such as, e.g., the possible contribution of sea quarks to the

nucleon properties such as spin, charge, and magnetic moment. Indeed, parity-violating scattering reactions can be used to probe this specific nucleonic property that remains concealed in parity-conserving processes. From the late 1990s onwards, parity-violating electron scattering (PVES) has become a tool for hadron physics research at various electron accelerator facilities, aiming to probe the strange-quark effects in proton structure [5–12]. In the first place, PVES is suitable for the strange electric and magnetic form factors. Radiative corrections heavily complicate the extraction of the strange contribution  $g_A^s$  to the axial form factor  $G_A$  from the data. The various PVES programs triggered many theoretical studies of the strangeness magnetic moment and charge radius of the nucleon. These calculations are performed in a rich variety of hadron models, yielding predictions for the strangeness parameters covering a wide range of values [13–21]. A recent review of the theoretical and experimental status can be found in Ref. [22].

Neutrino-nucleus reactions provide an alternative method of addressing the strangeness content of the nucleon. In contrast to PVES, extracting  $g_A^s$  is not subject to radiative corrections. Data for  $(\nu, N)$  and  $(\bar{\nu}, N)$  elastic-scattering cross sections were collected at BNL [23]. As carbon was used as target material, an accurate understanding of nuclear corrections is a prerequisite for reliably extracting the strange-quark matrix elements from the data. Examples of relativistic studies that deal with the issue of computing the nuclear corrections are the relativistic Fermi gas (RFG) model of Refs. [24,25] and the relativistic distorted-wave impulse approximation (RDWIA) models of Refs. [25–28]. As absolute cross-section measurements involving neutrinos are challenging, a lot of effort has been devoted to the study of cross-section ratios. Examples include the ratio of proton-to-neutron knockout in NC neutrino-nucleus interactions [26–31], the ratio of NC to charged-current (CC) cross sections [32–34] and the ratio of NC to CC neutrino-antineutrino asymmetries [27,35]. For these ratios, the effects of nuclear corrections nearly cancel, facilitating the extraction of viable strange-quark contributions.

In this article, we wish to show that the helicity asymmetry—also defined as a ratio of cross sections—is very sensitive to sea-quark contributions to the vector form factors.

\*Corresponding author: Jan.Ryckebusch@ugent.be

To this end, the conclusion that  $A_l$  remains relatively free of medium-related corrections is of crucial importance. We should point out that measuring polarization asymmetries at current neutrino facilities is extremely challenging. Still, we consider our findings as a valuable theoretical insight.

The outline of this article is as follows. In Sec. II we present the relativistic multiple-scattering Glauber approximation formalism for the description of the helicity asymmetry within NC neutrino-nucleus scattering processes. In Sec. III we present our results for  $A_l$  and pay particular attention to the influence of medium corrections and strangeness contributions. In Sec. IV we summarize our findings.

## II. FORMALISM

The expressions for neutrino and antineutrino quasielastic neutral-current (NC) reactions from nuclei that result in one emitted nucleon,  $\nu(\bar{\nu}) + A \rightarrow \nu(\bar{\nu}) + N + (A - 1)$ , are, e.g., derived in Ref. [4]. Within the one-boson exchange approximation the onefold differential cross section for a fixed neutrino energy reads

$$\frac{d\sigma}{dT_N} = \frac{M_N M_{A-1}}{(2\pi)^3 M_A} 4\pi^2 \int \sin\theta_l d\theta_l \int \sin\theta_N d\theta_N \times k_N f_{\text{rec}}^{-1} \sigma_M(v_L R_L + v_T R_T + h v_{T'} R_{T'}). \quad (1)$$

In this expression,  $M_N$  ( $T_N$ ) represents the mass (kinetic energy) of the ejected nucleon  $N$ , whereas  $M_A$  ( $M_{A-1}$ ) refers to the mass of the target (residual) nucleus. The outgoing nucleon momentum is  $\vec{k}_N$ ,  $f_{\text{rec}}$  is the recoil factor, and  $\sigma_M$  a Mott-like cross section, defined by

$$\sigma_M = \left[ \frac{G_F \cos(\theta_l/2) \varepsilon' M_Z^2}{\sqrt{2\pi} (Q^2 + M_Z^2)} \right]^2. \quad (2)$$

In this expression,  $G_F$  refers to the Fermi constant,  $\varepsilon'$  is the energy of the scattered lepton, and  $M_Z$  the mass of the  $Z$  boson. The four-momentum transfer is given by  $q^\mu = (\omega, \vec{q})$  and  $Q^2 = -q_\mu q^\mu$ . The direction of the scattered lepton (outgoing nucleon) is fixed by the angles  $\Omega_l$  ( $\Omega_N$ ). In Eq. (1), the helicity is  $h = -1$  ( $h = +1$ ) for neutrinos (antineutrinos). Expressions for the kinematic factors  $v_L, v_T, v_{T'}$  and the structure functions  $R_L, R_T, R_{T'}$  can be found in Ref. [4]. The expression in Eq. (1) involves an averaging over the ejectile's spin. When fixing the helicity  $h_N = \vec{\sigma}_N \cdot \vec{k}_N / |\vec{k}_N|$  of the ejectile, the following expression for the differential cross section emerges

$$\frac{d\sigma}{dT_N}(h_N) = \frac{M_N M_{A-1}}{(2\pi)^3 M_A} 4\pi^2 \int \sin\theta_l d\theta_l \int \sin\theta_N d\theta_N k_N f_{\text{rec}}^{-1} \sigma_M \times [v_L (R_L^o + h_N R_L^l) + v_T (R_T^o + h_N R_T^l) + h v_{T'} (R_{T'}^o + h_N R_{T'}^l)], \quad (3)$$

where the indices  $o$  and  $l$  refer to the unpolarized and longitudinally polarized responses, respectively. The responses  $R$  embody the effects of the nuclear dynamics. The basic quantity to be computed is the transition matrix element  $\langle J^\mu \rangle$ . Adopting the impulse approximation and an independent-

nucleon picture,  $\langle J^\mu \rangle$  can be expressed as

$$\langle J^\mu \rangle = \int d\vec{r} \bar{\phi}_F(\vec{r}) \hat{J}^\mu(\vec{r}) e^{i\vec{q}\cdot\vec{r}} \phi_B(\vec{r}), \quad (4)$$

where  $\phi_B$  and  $\phi_F$  are relativistic bound-state and scattering wave functions, and  $\hat{J}^\mu$  is the single-nucleon electroweak current operator. In this work, we adopt wave functions  $\phi_B$  as obtained within the Hartree approximation to the  $\sigma$ - $\omega$  model [36]. It is well-known that, even in a mean-field approximation, Fermi motion and the Pauli exclusion principle is taken into account.

For a free nucleon, the one-body vertex function  $\hat{J}^\mu$  can be expressed in several equivalent forms of which some of the more frequently used ones read [37]

$$\hat{J}_{cc1}^\mu = G_M^Z(Q^2) \gamma^\mu - \frac{\kappa}{2M_N} F_2^Z(Q^2) (K_i^\mu + K_f^\mu) + G_A(Q^2) \gamma^\mu \gamma_5, \quad (5a)$$

$$\hat{J}_{cc2}^\mu = F_1^Z(Q^2) \gamma^\mu + i \frac{\kappa}{2M_N} F_2^Z(Q^2) \sigma^{\mu\nu} q_\nu + G_A(Q^2) \gamma^\mu \gamma_5, \quad (5b)$$

$$\hat{J}_{cc3}^\mu = \frac{1}{2M_N} F_1^Z(Q^2) (K_i^\mu + K_f^\mu) + i \frac{1}{2M_N} G_M^Z(Q^2) \sigma^{\mu\nu} q_\nu + G_A(Q^2) \gamma^\mu \gamma_5. \quad (5c)$$

The relation between the weak Sachs electric and magnetic form factors  $G_E^Z$  and  $G_M^Z$  and the weak Dirac and Pauli form factors  $F_1^Z$  and  $F_2^Z$ , is established in the standard fashion. When considering off-shell nucleons embedded in a nuclear medium, the above vertex functions can no longer be guaranteed to produce identical results. This elusive feature is known as the Gordon ambiguity and is a source of uncertainties when performing calculations involving finite nuclei [37–41].

The weak vector form factors  $F_1^Z$  and  $F_2^Z$  can be expressed in terms of the electromagnetic form factors for protons ( $F_{i,p}^{EM}$ ) and neutrons ( $F_{i,n}^{EM}$ ) using the conserved vector current (CVC) hypothesis

$$F_i^Z = \left(\frac{1}{2} - \sin^2 \theta_W\right) (F_{i,p}^{EM} - F_{i,n}^{EM}) \tau_3 - \sin^2 \theta_W (F_{i,p}^{EM} + F_{i,n}^{EM}) - \frac{1}{2} F_i^s \quad (i = 1, 2), \quad (6)$$

with  $\sin^2 \theta_W = 0.2224$  the Weinberg angle and  $F_i^s$  quantifying the effect of the strange quarks. The isospin operator  $\tau_3$  equals  $+1$  ( $-1$ ) for protons (neutrons). For a long time, the accumulated data pointed toward electromagnetic form factors of the nucleon whose  $Q^2$  dependence could be well described in terms of a dipole parametrization. Traditionally, these data were obtained by means of a Rosenbluth separation of elastic  $p(e, e')p$  scattering measurements. New data based on polarization transfer measurements  $p(\vec{e}, e')\vec{p}$  [42,43] revealed quite a different picture for  $Q^2 \geq 1$  ( $\text{GeV}/c$ )<sup>2</sup>. The discrepancy between the electromagnetic form factors obtained with the two techniques is an unresolved issue, but two-photon exchange processes have been shown to play a major role [44,45].

The axial form factor is often parametrized in terms of a dipole

$$G_A(Q^2) = -\frac{(\tau_3 g_A - g_A^s)}{2} G(Q^2), \quad (7)$$

with  $g_A = 1.262$ ,  $G = (1 + Q^2/M^2)^{-2}$  with  $M = 1.032$  GeV, and  $g_A^s$  the axial strange-quark contribution.

The remaining ingredient entering Eq. (4) is the relativistic scattering wave function  $\phi_F$  for the emitted nucleon. We incorporate FSI effects in a relativistic version of the Glauber model which has been dubbed RMSGA [3]. The RMSGA represents a multiple-scattering extension of the eikonal approximation and the effects of FSI are directly computed from the elementary nucleon-nucleon scattering data. The Glauber method postulates linear trajectories for the ejectile and frozen spectator nucleons in the residual nucleus, resulting in a scattering wave function of the form

$$\phi_F(\vec{r}) \equiv \mathcal{G}[\vec{b}(x, y), z] \phi_{k_N, s_N}(\vec{r}), \quad (8)$$

where  $\phi_{k_N, s_N}$  is a relativistic plane wave. The impact of FSI mechanisms on the scattering wave function is contained in the scalar Dirac-Glauber phase  $\mathcal{G}(\vec{b}, z)$

$$\mathcal{G}(\vec{b}, z) = \prod_{\alpha \neq B} \left[ 1 - \int d\vec{r}' |\phi_\alpha(\vec{r}')|^2 \theta(z' - z) \Gamma(\vec{b} - \vec{b}') \right], \quad (9)$$

where the product over  $\alpha(n, \kappa, m)$  extends over all occupied single-particle states in the target nucleus, not including the one from which the nucleon is ejected. The profile function for  $NN$  scattering is defined in the standard manner

$$\Gamma(\vec{b}) = \frac{\sigma_{NN}^{\text{tot}}(1 - i\epsilon_{NN})}{4\pi\beta_{NN}^2} \exp\left(\frac{-b^2}{2\beta_{NN}^2}\right). \quad (10)$$

The parameters  $\sigma_{NN}^{\text{tot}}$ ,  $\beta_{NN}$ , and  $\epsilon_{NN}$  depend on the ejectile energy, and fitted values to the  $NN$  data can be found in Ref. [46]. The neutron-neutron scattering parameters are assumed identical to the proton-proton ones. The limit of vanishing FSI, i.e., the relativistic plane-wave impulse approximation (RPWIA), is reached by putting the Dirac-Glauber phase  $\mathcal{G}$  to unity. The RMSGA model was successfully tested against exclusive  $A(e, e'p)$  data [47,48]. In particular, inclusive quantities as the nuclear transparency received an overall good

description in a large energy range, underestimating the data by only roughly 5% [47]. A more stringent test that involved comparing the RMSGA predictions with exclusive  $A(\bar{\nu}, e' \bar{p})$  data also led to fair results [48]. Being a high-energy approximation, the validity of the RMSGA model for computing FSI mechanisms in neutrino-nucleus interactions was investigated by comparing its predictions to results of RDWIA calculations, which are typical low-energy frameworks [4]. Satisfactory RMSGA results down to nucleon kinetic energies of 250 MeV were found.

The longitudinal polarization asymmetry  $A_l$ , which will be the object of discussion in this article, is defined as the difference in yield for the two possible helicity states of the ejectile, normalized to the total differential nucleon knockout cross section:

$$A_l(T_N) = \frac{\frac{d\sigma}{dT_N}(h_N = +1) - \frac{d\sigma}{dT_N}(h_N = -1)}{\frac{d\sigma}{dT_N}(h_N = +1) + \frac{d\sigma}{dT_N}(h_N = -1)}, \quad (11)$$

where  $d\sigma/dT_N(h_N)$  was defined in Eq. (3).

### III. RESULTS

As mentioned earlier, in Ref. [1] the helicity asymmetry  $A_l$  was put forward as a lever to discriminate between neutrinos and antineutrinos in NC reactions on nuclei. Predictions for this asymmetry were obtained in a NRPWIA framework. First, we scrutinize the impact of effects, which are absent in the numerical calculations of Refs. [1,2], on the observable  $A_l$ . We wish to determine the degree to which  $A_l$  is affected by variations in the parametrizations for the electromagnetic form factors and typical medium effects such as FSI and off-shell ambiguities. We consider the  $^{12}\text{C}$  target as a test case. We take RPWIA calculations as baseline results, with dipole form factors and the current operator in the  $CC2$  form of Eq. (5b).

In Ref. [1], results up to beam energies of 500 MeV were presented. At impinging (anti-)neutrino energies of the order of GeVs, any realistic model for describing the reaction processes requires the inclusion of relativistic effects. In Fig. 1, we show the RPWIA predictions for  $A_l$  for beam energies ranging from 200 to 5000 MeV. Clearly, up to lepton energies of 1 GeV, the  $A_l$  has an opposite sign for  $A(\nu, N)$  and  $A(\bar{\nu}, N)$ .

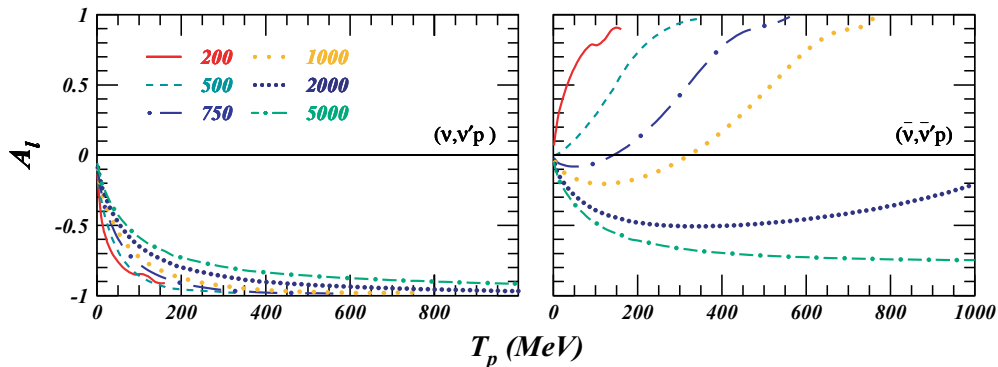


FIG. 1. (Color online) The helicity asymmetry as a function of  $T_p$  for proton knockout from  $^{12}\text{C}$  at six beam energies. The left (right) panel is for neutrinos (antineutrinos).

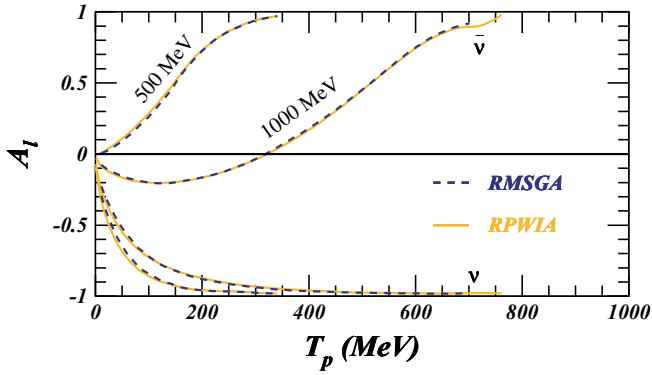


FIG. 2. (Color online) The effect of FSI mechanisms on the helicity asymmetry at 500 and 1000 MeV beam energies. The solid (dashed) line shows the RPWIA (RMSGGA) predictions.

Apparently, the discriminative power of  $A_l$  dwindles when higher beam energies are considered. The antineutrino proton asymmetry  $A_l(T_p)$  evolves from a dominance of  $h_N = +1$  contributions at beam energies below 1 GeV to a supremacy of  $h_N = -1$  ones at higher energies. This can be attributed to the role played by the  $G_A F_2^Z$  interference contribution, which gains in importance as the neutrino energy grows. The transverse response function  $R_T$  in the cross section of Eq. (1) becomes increasingly dominant when higher energies are probed, thereby extinguishing the distinction between left- and right-handed neutrino fields in the differential cross sections  $d\sigma/dT_N$ .

None of the results for  $A_l$  shown so far, including those of Refs. [1,2], did account for the effects of FSI. As already stated in the introduction, it is a common outcome of model calculations of various sorts that FSI do not play a major role in ratios of cross sections, albeit being important in the corresponding inclusive cross sections [4]. Figure 2 displays the effect of FSI mechanisms on  $A_l$  as computed in the RMSGGA model at impinging beam energies of 500 and 1000 MeV. As can be appreciated, the global influence of FSI mechanisms on  $A_l$  is indeed almost negligible. In the ratio  $A_l$ , a strong cancellation of FSI is noticed, even at relatively low

ejectile kinetic energies. Henceforth, we concentrate on results for an impinging (anti-)neutrino energy of  $\varepsilon = 1000$  MeV. At this energy, the neutrino scattering process can be expected to be dominated by the quasielastic contribution.

Another possible source of uncertainty when determining  $A_l$  may be the insufficient knowledge regarding the electromagnetic form factors of the proton. To this end, we performed calculations with two parametrizations: the standard dipole form and the recent BBA-2003 parametrization of Ref. [49]. As becomes clear from the left panel of Fig. 3, both produce comparable results. Therefore, all forthcoming results use the traditional dipole form for  $G_E^{EM}$  and  $G_M^{EM}$ . We also estimate the role of off-shell ambiguities on the computed  $A_l$  values. To that purpose we performed calculations with all current operators of Eq. (5). As becomes evident from Fig. 3, all these current operators produce almost equivalent results. Therefore, the sensitivity of  $A_l$  to off-shell ambiguities is minor.

The helicity asymmetry  $A_l$  emerges as a robust observable, which is not burdened by a large sensitivity to medium corrections. So far, we neglected strangeness contributions to the weak vector and axial form factors of Eqs. (6) and (7) ( $F_1^s = F_2^s = g_A^s = 0$ ). To quantify the impact of the axial strangeness contribution on  $G_A$ , we adopt the value  $g_A^s = -0.19$ , which we consider as an upper limit. Indeed,  $g_A^s = -0.19$  was extracted from an SU(3)-based analysis of deep inelastic double-polarized scattering experiments [50]. Recent neutrino and parity-violating electron scattering experiments point toward smaller values for  $g_A^s$  [23,51–53]. In addition to sea-quark effects in the axial current, there can be contributions to the Dirac and Pauli vector form factors. A three-pole ansatz of Forkel *et al.* [54] resulted in the following parametrization

$$F_1^s = \frac{1}{6} \frac{-r_s^2 Q^2}{(1 + Q^2/M_1^2)^2}, \quad (12)$$

$$F_2^s = \frac{\mu_s}{(1 + Q^2/M_2^2)^2}, \quad (13)$$

with  $M_1 = 1.3$  GeV and  $M_2 = 1.26$  GeV [54]. The  $r_s^2$  and  $\mu_s$  predicted by various hadronic structure models are summarized in Table I. The list is not exhaustive. There is

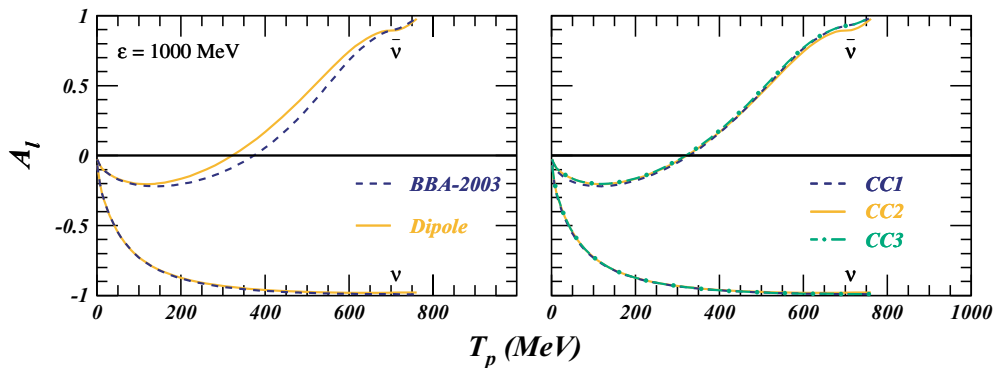


FIG. 3. (Color online) The helicity asymmetry  $A_l$  as a function of the proton kinetic energy at  $\varepsilon = 1000$  MeV as computed in an RPWIA approach. The left panel illustrates the effects stemming from the ambiguities in the electromagnetic form factors: the solid (dashed) line shows the RPWIA results obtained with the dipole (BBA-2003) parametrization. In the right panel the role of the off-shell ambiguities is studied. The solid, dashed, and dot-dashed curves are obtained with the CC2, CC1, and CC3 prescription, respectively.

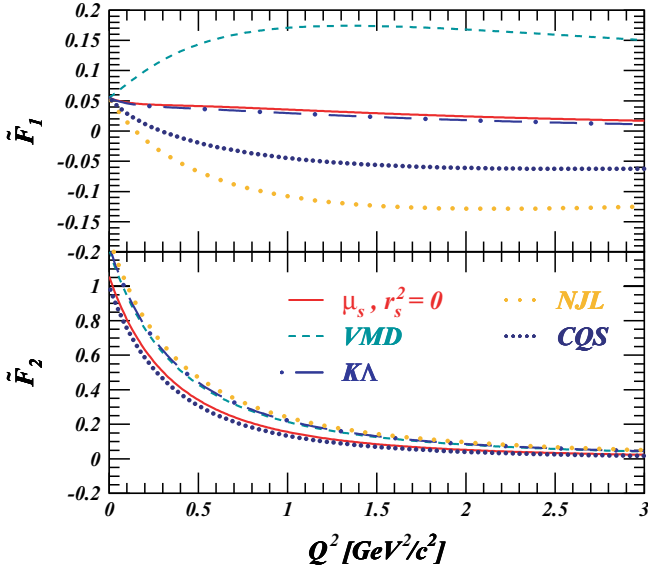


FIG. 4. (Color online) Sensitivity of the proton Dirac (upper panel) and Pauli (lower panel) neutral-current vector form factors to strange-quark contributions. The solid line represents the form factors in the absence of any strangeness contribution. The dashed, dot-dashed, long-dotted, and short-dotted curves include nonzero strangeness contributions in the parametrization of Eqs. (12) and (13). The adopted values for  $r_s^2$  and  $\mu_s$  are those of four different hadron models (VMD [13],  $K\Lambda$  [14], NJL [18], and CQS(K) model [21]) and can be found in Table I.

a tendency toward a mildly negative strangeness magnetic moment ( $\mu_s \approx -0.3 \mu_N$ ) and a small negative strangeness radius ( $r_s^2 \approx -0.01 \text{ fm}^2$ ). All PVES experiments performed so far, however, hint at a positive value for  $\mu_s$ . In our investigations we will use the predictions for  $r_s^2$  and  $\mu_s$  from the vector meson dominance (VMD), the  $K\Lambda$ , the Nambu-Jona-Lasinio (NJL) and the chiral quark soliton [CQS(K)] model. These values are selected as we find them representative for the theoretical predictions. Of those, the CQS(K) predictions for  $\mu_s$  and  $r_s^2$  are most realistic in light of the recent PVES results. We wish to stress that all forthcoming results for

TABLE I. Predictions for  $r_s^2$  and  $\mu_s$  in various hadron models.

Model	Ref.	$\mu_s (\mu_N)$	$r_s^2 (\text{fm}^2)$
VMD	[13]	-0.31	0.16
$K\Lambda$	[14]	-0.35	-0.007
CBM	[15]	-0.1	-0.011
Hybrid	[16]	-0.3	-0.025
Chiral quark	[17]	-0.09	-0.035
NJL	[18]	-0.45	-0.17
Skyrme	[19]	-0.13-0.57	-0.1-0.15
Disp. rel.	[20]	-0.28	0.42
CQS ( $\pi$ )	[21]	0.074	-0.220
CQS (K)	[21]	0.115	-0.095

the effect of strangeness in the weak vector form factors on  $A_l$ , account for strange sea-quark effects in the axial current. Hence, the interference between the axial and magnetic strange form factors is always present.

In Fig. 4, the proton Dirac  $F_1^Z$  and Pauli  $F_2^Z$  NC form factors are shown for various parametrizations for  $F_1^s$  and  $F_2^s$ . The solid line provides the value in the absence of strangeness contributions. This figure reveals that mainly  $F_1^Z$  is affected. The VMD model predicts that strangeness mechanisms increase  $F_1^Z$  by about a factor of 3. All other models lead to less spectacular modifications in the absolute magnitude. The relatively large and negative  $r_s^2$  values from the NJL and CQS(K) nucleon models make the strangeness parts to change the sign of  $F_1^Z$ . Strangeness effects for the Pauli form factor  $F_2^Z$  are far less pronounced because of its large absolute value. Thus, one can expect that mainly variations in  $r_s^2$  will be reflected in the helicity asymmetry.

Figure 5 shows our predictions for the helicity asymmetry at  $\varepsilon = 1000 \text{ MeV}$  for both proton and neutron knockout in  $\bar{\nu}$ - $^{12}\text{C}$  reactions. The results contained in Figs. 1, 2, and 3 reveal that neutrinos are extremely selective with respect to the helicity of the ejectile. As a consequence, one can expect that any strangeness contribution will nearly cancel in the ratio of Eq. (11). The helicity selectivity is not so pronounced for antineutrinos. Hence, antineutrinos represent a better

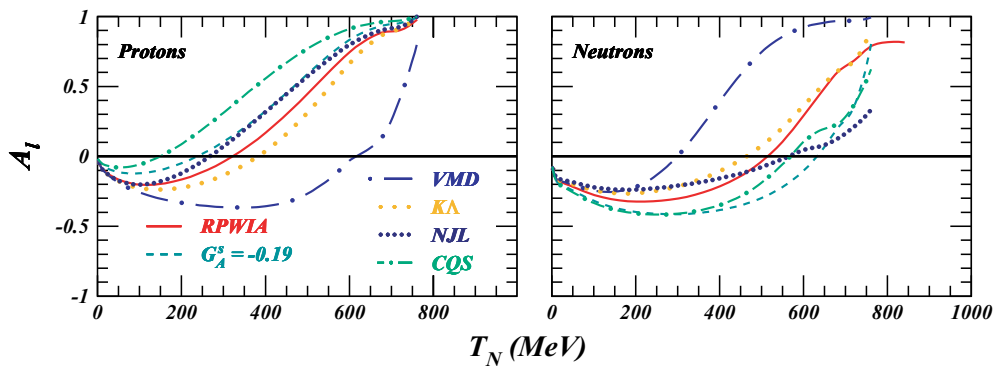


FIG. 5. (Color online) Influence of sea-quarks on the helicity asymmetry at  $\varepsilon = 1000 \text{ MeV}$ . The left panel shows the asymmetry for antineutrino-induced proton knockout on  $^{12}\text{C}$ , whilst the right one shows the asymmetry for antineutrino-induced neutron knockout. The solid curve represents the RPWIA results without strangeness. The other curves adopt  $g_A^s = -0.19$  and correspond to different values for  $r_s^2$  and  $\mu_s$ : ( $r_s^2 = 0, \mu_s = 0$ ) (dashed), VMD (long dot-dashed) [13],  $K\Lambda$  (long-dotted) [14], NJL (short-dotted) [18], and CQS(K) (short dot-dashed) [21].

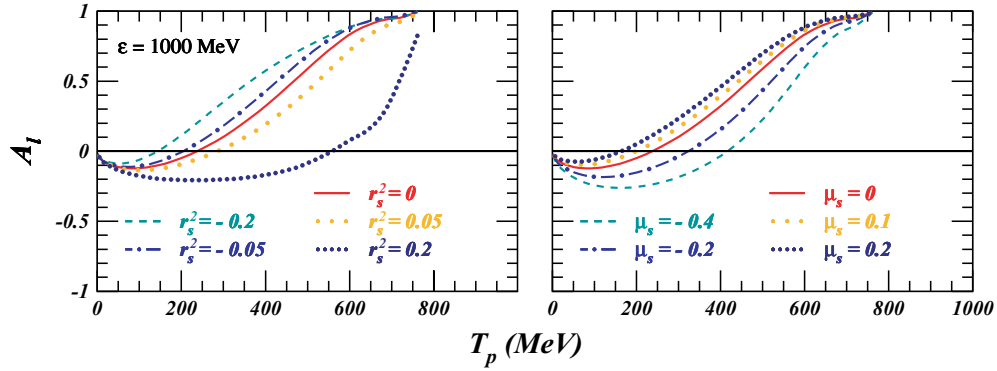


FIG. 6. (Color online) The helicity asymmetry for antineutrino-induced proton knockout from  $^{12}\text{C}$  at  $\varepsilon = 1000$  MeV. The solid line shows the RPWIA predictions with  $g_A^s = -0.19$ . The left (right) panel illustrates the predicted effect of varying the strangeness radius (magnetic moment).

lever than neutrinos when it comes to probing strange-quark contributions through the observable  $A_l$ . For both protons and neutrons, the introduction of a nonzero  $g_A^s$  does not substantially alter the baseline results (denoted as RPWIA in the figure). The introduction of a nonzero strangeness radius and magnetic moment, however, seriously affects the ratio between  $h_N = +1$  and  $h_N = -1$  ejectiles. The largest deviations emerge using the predictions of the VMD model ( $r_s^2 > 0$ ). In any case, the overall impact of  $F_1^s$  and  $F_2^s$  on the helicity asymmetry is substantially larger than the combined effect from FSI, off-shell ambiguities and  $g_A^s$ . We stress that for  $g_A^s$  an upper limit is adopted. Considering that recent PVES and neutrino-scattering processes point toward smaller values for  $g_A^s$  [23,51–53], one can conclude that the impact of  $g_A^s$  on  $A_l$  is extremely small. As can be inferred from Fig. 5, the strange contribution to the weak vector form factors has a comparable impact on the  $A_l$  for protons and neutrons but acts in opposite directions. This is another illustration of the well-known feature that in hunting sea-quarks in neutrino or PVES reactions, it is essential to discriminate between protons and neutrons. Indeed, the effects stemming from the sea quarks tend to cancel when performing a summation over the proton and neutron observables.

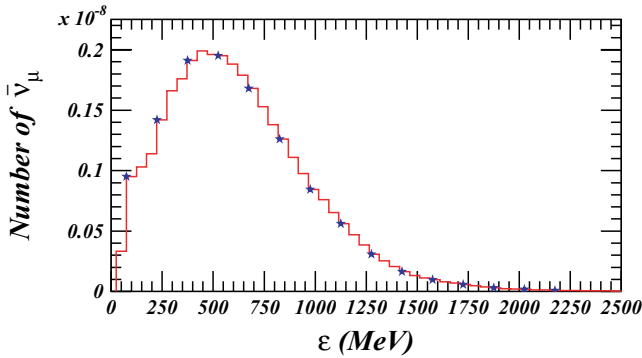


FIG. 7. (Color online) A typical FINeSSE antineutrino flux on the FNAL booster Neutrino beamline [55]. Units are  $\bar{\nu}_\mu$  per protons on target per  $\text{cm}^2$  per 50 MeV. The average beam energy corresponds to  $\langle \varepsilon \rangle \approx 600$  MeV. The stars indicate the energies for which calculations were performed.

The effect of varying  $r_s^2$  and  $\mu_s$  independently is studied in Fig. 6. In the right panel, we investigate the effect of varying  $\mu_s$  at  $r_s = 0$ . The left panel, however, displays the effect of varying  $r_s^2$  at  $\mu_s = 0$ . From the theoretical predictions listed in Table I one infers a range of values  $-0.4 \lesssim \mu_s \lesssim 0.2$  and  $-0.22 \lesssim r_s^2 \lesssim 0.42$ . Figure 6 illustrates that the largest changes in  $A_l$  are induced by variations in the strangeness radius  $r_s^2$ .

Figure 1 revealed that the helicity asymmetry is very sensitive to the energy of the (anti-)neutrino beam. Any experiment involving neutrinos has limited capabilities to precisely determine the initial (anti-)neutrino energies. Therefore, we investigated to what extent the sensitivity of  $A_l$  to strangeness effects persists when it is folded over a realistic antineutrino spectrum. To this end, we have computed  $A_l$  as a function of the proton energy as it could be determined at an experiment like FINeSSE, provided that it possesses the capabilities to determine outgoing nucleon helicities. A typical beam spectrum of FINeSSE is displayed in Fig. 7 [55]. The average beam energy corresponds to  $\langle \varepsilon \rangle \approx 600$  MeV. The flux-averaged differential cross section is defined as

$$\left\langle \frac{d\sigma}{dT_N}(h_N) \right\rangle = \frac{\int_{\varepsilon_{\min}}^{\varepsilon_{\max}} \Phi(\varepsilon) \frac{d\sigma}{dT_N}(\varepsilon, h_N) d\varepsilon}{\int_{\varepsilon_{\min}}^{\varepsilon_{\max}} \Phi(\varepsilon) d\varepsilon}, \quad (14)$$

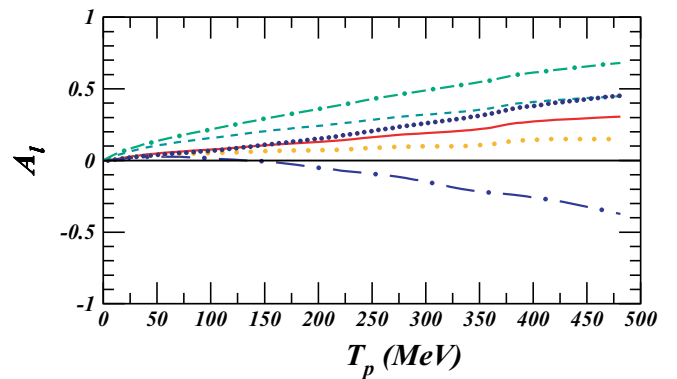


FIG. 8. (Color online) The flux-averaged helicity asymmetry for antineutrino-induced proton knockout at  $\langle \varepsilon \rangle = 600$  MeV. Line conventions as in Fig. 5.

with  $\Phi(\varepsilon)$  the typical FINeSSE antineutrino spectrum of Fig. 7,  $\varepsilon_{\min} = 75$  MeV and  $\varepsilon_{\max} = 2375$  MeV.

Figure 8 shows the flux-averaged helicity asymmetry for antineutrino-induced proton knockout from  $^{12}\text{C}$ . The strange-quark effects remain substantial for the flux-averaged  $A_l$  and similar trends emerge as those observed in Fig. 5 which refers to a well-defined impinging antineutrino energy. For the  $Q^2$  ranges of our presented results, the impact of the adopted values for  $M_1$  and  $M_2$  in Eqs. (12) and (13) is nearly negligible.

#### IV. CONCLUSIONS

We have studied the helicity properties of the ejectile in quasielastic neutrino-induced nucleon-knockout reactions. We scrutinized on the impact of effects that were absent in the pioneering work of Refs. [1,2]. Results for  $^{12}\text{C}$  have been presented for a wide range of (anti-)neutrino energies. The

nucleon helicity asymmetry  $A_l$  is found to be hardly affected by nuclear structure effects, such as final-state interactions, form-factor parametrization, and off-shell ambiguities in the electroweak current operators. Hence, we were tempted to address more exotic effects. In particular, in  $A(\bar{\nu}, N)$  processes, the helicity asymmetry appears to be very sensitive to strangeness contributions in the weak Dirac and Pauli form factors.

#### ACKNOWLEDGMENTS

We are grateful to S. Pate for providing us with a typical FINeSSE antineutrino flux. This work is supported by the Fund for Scientific Research Flanders and the Research Board of Ghent University. M.C.M. acknowledges postdoctoral financial support from the Ministerio de Educacion y Ciencia (MEC) of Spain.

- 
- [1] N. Jachowicz, K. Vantournhout, J. Ryckebusch, and K. Heyde, *Phys. Rev. Lett.* **93**, 082501 (2004).
- [2] N. Jachowicz, K. Vantournhout, J. Ryckebusch, and K. Heyde, *Phys. Rev. C* **71**, 034604 (2005).
- [3] J. Ryckebusch, D. Debruyne, P. Lava, S. Janssen, B. Van Overmeire, and T. Van Cauteren, *Nucl. Phys.* **A728**, 226 (2003).
- [4] M. C. Martínez, P. Lava, N. Jachowicz, J. Ryckebusch, K. Vantournhout, and J. M. Udías, *Phys. Rev. C* **73**, 024607 (2006).
- [5] B. A. Mueller *et al.*, *Phys. Rev. Lett.* **78**, 3824 (1997).
- [6] K. Aniol *et al.*, *Phys. Rev. Lett.* **82**, 1096 (1999).
- [7] K. Aniol *et al.*, *Phys. Rev. C* **69**, 065501 (2004).
- [8] K. Aniol *et al.*, *Phys. Rev. Lett.* **96**, 022003 (2006).
- [9] D. S. Armstrong *et al.*, *Phys. Rev. Lett.* **95**, 092001 (2005).
- [10] F. E. Maas *et al.*, *Phys. Rev. Lett.* **93**, 022002 (2004).
- [11] F. E. Maas *et al.*, *Phys. Rev. Lett.* **94**, 152001 (2005).
- [12] P. L. Anthony *et al.*, *Phys. Rev. Lett.* **92**, 181602 (2004).
- [13] R. L. Jaffe, *Phys. Lett.* **B229**, 275 (1989).
- [14] M. J. Ramsey-Musolf and M. Burkardt, *Z. Phys. C* **61**, 433 (1994).
- [15] W. Koepf, S. J. Pollock, and E. M. Henley, *Phys. Lett.* **B288**, 11 (1992).
- [16] T. Cohen, H. Forkel, and M. Nielsen, *Phys. Lett.* **B316**, 1 (1993).
- [17] M. J. Ramsey-Musolf and H. Ito, *Phys. Rev. C* **55**, 3066 (1997).
- [18] H. C. Kim, T. Watabe, and K. Goeke, *Nucl. Phys.* **A616**, 606 (1997); H. Weigel, A. Abada, R. Alkofer, and H. Reinhardt, *Phys. Lett.* **B353**, 20 (1995).
- [19] N. W. Park, J. Schechter, and H. Weigel, *Phys. Rev. D* **43**, 869 (1991).
- [20] M. J. Musolf, H.-W. Hammer, and D. Drechsel, *Phys. Rev. D* **55**, 2741 (1997).
- [21] A. Silva, H. C. Kim, and K. Goeke, *Phys. Rev. D* **65**, 014016 (2001).
- [22] M. J. Ramsey-Musolf, *Eur. Phys. J. A* **24S2**, 197 (2005).
- [23] L. A. Ahrens *et al.*, *Phys. Rev. D* **35**, 785 (1987).
- [24] C. J. Horowitz, H. Kim, D. P. Murdock, and S. Pollock, *Phys. Rev. C* **48**, 3078 (1993).
- [25] W. M. Alberico, M. B. Barbaro, S. M. Bilenky, J. A. Caballero, C. Giunti, C. Maieron, E. Moya de Guerra, and J. M. Udias, *Nucl. Phys.* **A623**, 471 (1997).
- [26] W. M. Alberico, M. B. Barbaro, S. M. Bilenky, J. A. Caballero, C. Giunti, C. Maieron, E. Moya de Guerra, and J. M. Udias, *Phys. Lett.* **B438**, 9 (1998).
- [27] W. M. Alberico, S. M. Bilenky, and C. Maieron, *Phys. Rep.* **358**, 227 (2002).
- [28] A. Meucci, C. Giusti, and F. D. Pacati, *Nucl. Phys.* **A744**, 307 (2004).
- [29] W. M. Alberico, M. B. Barbaro, S. M. Bilenky, J. A. Caballero, C. Giunti, C. Maieron, E. Moya de Guerra, and J. M. Udias, *Nucl. Phys.* **A651**, 277 (1999).
- [30] G. Garvey, E. Kolbe, K. Langanke, and S. Krewald, *Phys. Rev. C* **48**, 1919 (1993).
- [31] B. I. S. van der Ventel and J. Piekarewicz, *Phys. Rev. C* **69**, 035501 (2004).
- [32] S. F. Pate, *Eur. Phys. J. A* **24S2**, 67 (2005).
- [33] B. I. S. van der Ventel and J. Piekarewicz, *Phys. Rev. C* **73**, 025501 (2006).
- [34] A. Meucci, C. Giusti, and F. D. Pacati, *nucl-th/0601052*.
- [35] W. M. Alberico, S. M. Bilenky, C. Giunti, and C. Maieron, *Z. Phys. C* **70**, 463 (1996).
- [36] B. D. Serot and J. D. Walecka, *Adv. Nucl. Phys.* **16**, 1 (1986).
- [37] T. de Forest, *Nucl. Phys.* **A392**, 232 (1983).
- [38] S. Pollock, H. W. L. Naus, and J. Koch, *Phys. Rev. C* **53**, 2304 (1996).
- [39] J. J. Kelly, *Phys. Rev. C* **56**, 2672 (1997).
- [40] J. A. Caballero, T. W. Donnelly, and G. I. Poulis, *Nucl. Phys.* **A555**, 709 (1993).
- [41] M. B. Barbaro, A. De Pace, T. W. Donnelly, A. Molinari, and M. J. Musolf, *Phys. Rev. C* **54**, 1954 (1996).
- [42] M. K. Jones *et al.*, *Phys. Rev. Lett.* **84**, 1398 (2000).
- [43] O. Gayou *et al.*, *Phys. Rev. Lett.* **88**, 092301 (2002).
- [44] P. A. M. Guichon and M. Vanderhaeghen, *Phys. Rev. Lett.* **91**, 142303 (2003).
- [45] P. G. Blunden, W. Melnitchouk, and J. A. Tjon, *Phys. Rev. Lett.* **91**, 142304 (2003).

- [46] Particle Data Group, K. Hagiwara *et al.*, Phys. Rev. D **66**, 010001 (2002), <http://pdg.lbl.gov/>
- [47] P. Lava, M. C. Martínez, J. Ryckebusch, J. A. Caballero, and J. M. Udías, Phys. Lett. **B595**, 177 (2004).
- [48] P. Lava, J. Ryckebusch, B. Van Overmeire, and S. Strauch, Phys. Rev. C **71**, 014605 (2005).
- [49] H. Budd, A. Bodek, and J. Arrington, hep-ex/0308005; J. Arrington, Phys. Rev. C **69**, 022201(R) (2004).
- [50] J. Ashman *et al.*, Nucl. Phys. **B328**, 1 (1989).
- [51] B. Adeva *et al.*, Phys. Rev. D **58**, 112002 (1998).
- [52] P. L. Anthony *et al.*, Phys. Lett. **B493**, 19 (2000).
- [53] A. Airapetian *et al.*, Phys. Rev. Lett. **92**, 012005 (2004); Phys. Rev. D **71**, 012003 (2005).
- [54] H. Forkel, Phys. Rev. C **56**, 510 (1997).
- [55] S. Pate (private communication).